

See discussions, stats, and author profiles for this publication at: <https://www.researchgate.net/publication/7911214>

# Cobalt(III) Corroles as Electrocatalysts for the Reduction of Dioxygen: Reactivity of a Monocorrole, Biscorroles, and Porphyrin–Corrole Dyads

ARTICLE in JOURNAL OF THE AMERICAN CHEMICAL SOCIETY · MAY 2005

Impact Factor: 12.11 · DOI: 10.1021/ja0501060 · Source: PubMed

CITATIONS

109

READS

65

10 AUTHORS, INCLUDING:



Laurent Fremond

12 PUBLICATIONS 332 CITATIONS

SEE PROFILE



Jean-Michel Barbe

University of Burgundy

157 PUBLICATIONS 3,001 CITATIONS

SEE PROFILE



Roger Guillard

University of Burgundy

486 PUBLICATIONS 8,484 CITATIONS

SEE PROFILE

## Cobalt(III) Corroles as Electrocatalysts for the Reduction of Dioxygen: Reactivity of a Monocorrole, Biscorroles, and Porphyrin–Corrole Dyads

Karl M. Kadish,<sup>\*,†</sup> Laurent Frémond,<sup>†</sup> Zhongping Ou,<sup>†</sup> Jianguo Shao,<sup>†</sup>  
Chunnian Shi,<sup>‡</sup> Fred C. Anson,<sup>‡</sup> Fabien Burdet,<sup>§</sup> Claude P. Gros,<sup>§</sup>  
Jean-Michel Barbe,<sup>§</sup> and Roger Guillard<sup>\*,§</sup>

*Contribution from the Department of Chemistry, University of Houston,  
Houston, Texas 77204-5003, Division of Chemistry and Chemical Engineering, Arthur Amos  
Noyes Laboratory, California Institute of Technology, Pasadena, California 91125, and  
Université de Bourgogne, LIMSAG (UMR 5633), 6 boulevard Gabriel, 21100 Dijon, France*

Received January 7, 2005; E-mail: kkadish@uh.edu; rguillard@u-bourgogne.fr

**Abstract:** Three series of cobalt(III) corroles were tested as catalysts for the electroreduction of dioxygen to water. One was a simple monocorrole represented as (Me<sub>4</sub>Ph<sub>5</sub>Cor)Co, one a face-to-face biscorrole linked by an anthracene (A), biphenylene (B), 9,9-dimethylxanthene (X), dibenzofuran (O) or dibenzothiophene (S) bridge, (BCY)Co<sub>2</sub> (with Y = A, B, X, O or S), and one a face-to-face bismacrocylic complex, (PCY)Co<sub>2</sub>, containing a Co(II) porphyrin and a Co(III) corrole also linked by one of the above rigid spacers (Y = A, B, X, or O). Cyclic voltammetry and rotating ring–disk electrode voltammetry were both used to examine the catalytic activity of the cobalt complexes in acid media. The mixed valent Co(II)/Co(III) complexes, (PCY)Co<sub>2</sub>, and the biscorrole complexes, (BCY)Co<sub>2</sub>, which contain two Co(III) ions in their air-stable forms, all provide a direct four-electron pathway for the reduction of O<sub>2</sub> to H<sub>2</sub>O in aqueous acidic electrolyte when adsorbed on a graphite electrode, with the most efficient process being observed in the case of the complexes having an anthracene spacer. A relatively small amount of hydrogen peroxide was detected at the ring electrode in the vicinity of E<sub>1/2</sub> which was located at 0.47 V vs SCE for (PCA)Co<sub>2</sub> and 0.39 V vs SCE for (BCA)Co<sub>2</sub>. The cobalt(III) monocorrole (Me<sub>4</sub>Ph<sub>5</sub>Cor)Co also catalyzes the electroreduction of dioxygen at E<sub>1/2</sub> = 0.38 V with the final products being an approximate 50% mixture of H<sub>2</sub>O<sub>2</sub> and H<sub>2</sub>O.

### Introduction

Several porphyrin–corrole,<sup>1</sup> biscorrole,<sup>1</sup> and bisporphyrin<sup>2–8</sup> dyads linked in a cofacial configuration have been synthesized and examined as to their electrochemical reactivity with small molecules such as O<sub>2</sub> or CO. One such compound is the anthracenyl-bridged porphyrin–corrole dyad (PCA)Co<sub>2</sub>, **1a**, (Chart 1) which strongly binds O<sub>2</sub> in air giving a stable bis-Co(III)  $\mu$ -superoxo complex as evidenced by its 15-line ESR spectrum.<sup>9</sup> A similar dicobalt face-to-face anthracenyl-bridged

bisporphyrin<sup>2,10</sup> is able to catalyze the four-electron electroreduction of O<sub>2</sub> in acidic media, and it was of interest to examine catalytic properties of the related mixed oxidation state porphyrin–corrole dyads **1a–1d** and the Co(III) biscorrole dyads **3a–3e** (Chart 1) under similar experimental conditions.

Metallocorroles have been examined as to their catalytic properties in oxidation reactions<sup>11,12</sup> and their affinity for dioxygen,<sup>13</sup> but nothing has been reported as to their ability to catalyze the electroreduction of O<sub>2</sub> when adsorbed on an electrode surface. The main difference between the cobalt corroles and previously studied cobalt porphyrins is the oxidation state of the central metal ion. The uncharged cobalt mono- and bisporphyrins contain Co(II) ions, while the neutral porphyrin–corrole dyads, **1a–1d**, contain a Co(III) corrole linked to a Co(II) porphyrin. In contrast, the biscorrole dyads (BCY)Co<sub>2</sub>, **3a–3e**, and the uncharged monocorrole **2** contain only Co(III) ions.

One goal of the present study was to examine the redox properties of the three series of corroles in acidic media and

<sup>†</sup> University of Houston.

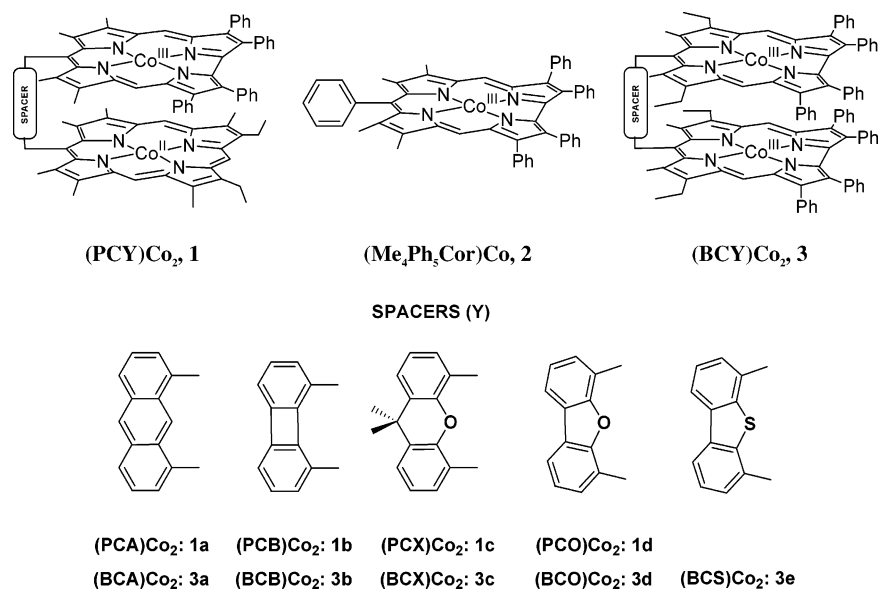
<sup>‡</sup> California Institute of Technology.

<sup>§</sup> Université de Bourgogne.

- (1) Guillard, R.; Barbe, J.-M.; Stern, C.; Kadish, K. M. In *The Porphyrin Handbook*; Kadish, K. M., Smith, J. R. L., Guillard, R., Eds.; Academic Press: Boston, 2003; Vol. 18, pp 303–349.
- (2) Collman, J. P.; Boulatov, R.; Sunderland, C. J. *The Porphyrin Handbook*; Academic Press: Boston, 2003; Vol. 11, pp 1–49.
- (3) Le Mest, Y.; L'Her, M.; Hendricks, N. H.; Kim, K.; Collman, J. P. *Inorg. Chem.* **1992**, *31*, 835–847.
- (4) Le Mest, Y.; L'Her, M. *J. Chem. Soc., Chem. Commun.* **1995**, 1441–1442.
- (5) Le Mest, Y.; L'Her, M.; Saillard, J.-Y. *Inorg. Chim. Acta* **1996**, *248*, 181–191.
- (6) Le Mest, Y.; Inisan, C.; Laouenan, A.; L'Her, M.; Talarmin, J.; El Khalifa, M.; Saillard, J.-Y. *J. Am. Chem. Soc.* **1997**, *119*, 6095–6106.
- (7) Chang, C. J.; Loh, Z.-H.; Shi, C.; Anson, F. C.; Nocera, D. G. *J. Am. Chem. Soc.* **2004**, *126*, 10013–10020.
- (8) Collman, J. P.; Wagenknecht, P. S.; Hutchison, J. E. *Angew. Chem., Int. Ed. Engl.* **1994**, *33*, 1537–1554.
- (9) Guillard, R.; Jérôme, F.; Gros, C. P.; Barbe, J.-M.; Ou, Z.; Shao, J.; Kadish, K. M. *C. R. Acad. Sci., Ser. IIc: Chim.* **2001**, *4*, 245–254.

- (10) Chang, C. K.; Liu, H.-Y.; Abdalmuhdi, I. *J. Am. Chem. Soc.* **1984**, *106*, 2725–2726.
- (11) Collman, J. P.; Zeng, L.; Decreau, R. A. *Chem. Commun.* **2003**, *24*, 2974–2975.
- (12) Mahammed, A.; Gray, H. B.; Meier-Callahan, A. E.; Gross, Z. *J. Am. Chem. Soc.* **2003**, *125*, 1162–1163.
- (13) Ramdhanie, B.; Telser, J.; Caneschi, A.; Zakharov, L. N.; Rheingold, A. L.; Goldberg, D. P. *J. Am. Chem. Soc.* **2004**, *126*, 2515–2525.

Chart 1



another was to examine their use as catalysts for the reduction of O<sub>2</sub> at a graphite electrode. All 10 corroles examined in this study are well characterized as to their electrochemistry under N<sub>2</sub> in a variety of nonaqueous solvents.<sup>9,14–17</sup> (Me<sub>4</sub>Ph<sub>5</sub>Cor)-Co<sup>III</sup>, **2**, can be reversibly reduced to its Co(II) form at  $E_{1/2} = -0.15$  to  $-0.17$  V vs SCE in CH<sub>2</sub>Cl<sub>2</sub>, PhCN, or THF.<sup>14</sup> Slightly more negative potentials are observed for the Co(III)/Co(II) process of the biscalcoroles (BCY)Co<sub>2</sub><sup>15,16</sup> and porphyrin–corroles (PCY)Co<sub>2</sub><sup>15</sup> under similar experimental conditions.

Of more relevance to the present work are the potentials where the three investigated corroles are oxidized to their higher, formally Co(IV) and Co(IV)  $\pi$ -cation radical oxidation states. These electrode reactions occur at  $E_{1/2} = 0.47$  and  $0.82$  V for (Me<sub>4</sub>Ph<sub>5</sub>Cor)Co<sup>III</sup>, **2**, in PhCN 0.1 M TBAP and at  $E_{1/2} = 0.53$  and  $0.73$  V in THF giving [2]<sup>+</sup> and [2]<sup>2+</sup> in both solvents.<sup>14</sup> A splitting of the first redox process of **2** is observed in CH<sub>2</sub>Cl<sub>2</sub> due to the presence of dimers.<sup>14</sup> As will be described, both series of biscobalt complexes **1** and **3** can serve as catalysts for the four-electron electroreduction of dioxygen in an air-saturated aqueous acidic solution containing 1 M HClO<sub>4</sub>. The onset potentials of the catalytic reduction for both biscobalt complexes are comparable to the potentials for the formal Co(IV)/Co(III) processes of the catalysts in nonaqueous media. This result is consistent with the binding of O<sub>2</sub> by the Co(III) form of the compounds and is also consistent with the previously described  $\mu$ -superoxo species that are formed in the reaction between O<sub>2</sub> and (PCA)Co<sub>2</sub>.<sup>9</sup>

## Experimental Section

**Chemicals and Corroles.** Unless otherwise noted, all chemicals were obtained commercially and used without further purification. High-purity N<sub>2</sub> gas was purchased from Matheson-Trigas. Organic solvents and mineral acids were of reagent grade and were used as supplied

except for benzonitrile (PhCN) which was purified by passage through a column of activated Linde 3 Å molecular sieves followed by distillation under reduced pressure. All subsequent aqueous solutions were prepared with deionized water of resistivity not less than 18 MΩ cm. The synthesis and characterization of the cobalt complexes used in this study [(PCY)Co<sub>2</sub>, (BCY)Co<sub>2</sub>, and (Me<sub>4</sub>Ph<sub>5</sub>Cor)Co] were reported elsewhere.<sup>15,18</sup> Thin layers of PhCN separating the polished edge-plane pyrolytic graphite electrode from aqueous acidic solutions were prepared and utilized according to procedures described in the literature.<sup>19</sup>

**Electrochemical Apparatus and Procedures.** All electrochemical data were collected using a three-electrode cell. The three-electrode system consisted of a platinum ring–graphite disk working electrode, a platinum wire as the auxiliary electrode, and a commercial saturated calomel electrode (SCE) as the reference which was separated from the bulk of the solution by means of a salt bridge. The KCl solution in the SCE was changed periodically to maintain the correct potential that was checked using a standard solution for redox potential measurements.<sup>20</sup> An aqueous Ag/AgCl/3 M NaCl reference electrode ( $-40$  mV vs SCE) was employed for thin-layer experiments.

All electrochemical experiments were conducted at ambient laboratory temperature ( $22 \pm 2$  °C). Cyclic voltammetry and rotating disk experiments were carried out using a Pine Instrument model AFMSR rotator linked to an EG&G Princeton Applied Research (PAR) model 263A potentiostat/galvanostat. The potentiostat was monitored by an IBM-compatible PC microcomputer controlled by the software M270 (EG&G PARC). A RDE4 bipotentiostat (Pine Instrument) was employed with a HP 7090A three-channel digital plotter for rotating ring–disk electrochemical experiments. The rotating ring–disk electrode (RRDE), purchased from the Pine Instrument Co., consisted of a platinum ring and a removable graphite disk.

The equations used to calculate the average number of electrons transferred  $n$  and the percentage of H<sub>2</sub>O<sub>2</sub> formed at the electrode are  $n = 4I_D/(I_D + I_R/N)$  and % H<sub>2</sub>O<sub>2</sub> =  $100(2I_R/N)/(I_D + I_R/N)$ , respectively, where  $I_D$  is the faradic current at the disk and  $I_R$  is the faradic current at the ring.<sup>21</sup> The intrinsic value of the collection efficiency was determined to be  $N = 0.24$  using the Fe(CN)<sub>6</sub><sup>3-/4-</sup> redox couple in 1 M KCl. Just before it was coated with the catalyst, the edge-plane pyrolytic graphite disk ( $A = 0.282$  cm<sup>2</sup>) was polished to a rough finish

(14) Kadish, K. M.; Shao, J.; Ou, Z.; Gros, C. P.; Bolze, F.; Barbe, J.-M.; Guillard, R. *Inorg. Chem.* **2003**, *42*, 4062–4070.

(15) Kadish, K. M.; Ou, Z.; Shao, J.; Gros, C. P.; Barbe, J.-M.; Jérôme, F.; Bolze, F.; Burdet, F.; Guillard, R. *Inorg. Chem.* **2002**, *41*, 3990–4005.

(16) Guillard, R.; Jérôme, F.; Barbe, J.-M.; Gros, C. P.; Ou, Z.; Shao, J.; Fischer, J.; Weiss, R.; Kadish, K. M. *Inorg. Chem.* **2001**, *40*, 4856–4865.

(17) Guillard, R.; Gros, C. P.; Bolze, F.; Jérôme, F.; Ou, Z.; Shao, J.; Fischer, J.; Weiss, R.; Kadish, K. M. *Inorg. Chem.* **2001**, *40*, 4845–4855.

(18) Barbe, J.-M.; Burdet, F.; Espinosa, E.; Gros, C. P.; Guillard, R. J. *J. Porphyrins Phthalocyanines* **2003**, *7*, 365–374.

(19) Shi, C.; Anson, F. C. *Anal. Chem.* **1998**, *70*, 3114–3118.

(20) Light, T. S. *Anal. Chem.* **1972**, *44*, 1038–1039.

(21) Lefevre, M.; Dodelet, J.-P. *Electrochim. Acta* **2003**, *48*, 2749–2760.

with 600 grit SiC paper, rinsed with water, and wiped off to remove any free graphite particles. The molecular catalyst was irreversibly adsorbed on the electrode surface by means of a dip-coating procedure; the freshly polished electrode was dipped for 5 s in a 0.1 mM solution of the catalyst in  $\text{CHCl}_3$ , transferred rapidly to pure  $\text{CHCl}_3$  for 1–2 s, and then dried.<sup>22</sup> After coating, the ring–disk electrode was introduced into air-saturated aqueous acid 1 M  $\text{HClO}_4$ . Particular care was exercised to ensure high reactivity of the Pt ring toward  $\text{H}_2\text{O}_2$ . Immediately prior to use, Pt was cleaned with a 5- $\mu\text{m}$  alumina slurry (Buehler MICROPOLISH II polishing suspension) on a polishing cloth (Buehler MICROCLOTH), rinsed successively with water and methanol, dried, and activated by cycling between 1.20 and  $-0.24$  V in 1 M  $\text{HClO}_4$  until reproducible voltammograms were obtained.<sup>23,24</sup> During polishing of the Pt ring, the graphite disk was removed to avoid contamination of the Pt with graphite particles and to preserve the integrity of the graphite surface.

For  $(\text{Me}_4\text{Ph}_5\text{Cor})\text{Co}$ - and  $(\text{PCA})\text{Co}_2$ -catalyzed dioxygen reduction, the slopes of the Koutecký–Levich plots were determined by linear regression analysis of data acquired at 100, 400, 900, 1600, 2500, and 3600 rpm (rpm = revolutions per minute). The diffusion-limiting currents for the reduction of  $\text{O}_2$  in aqueous solution at the rotating disk electrode were calculated using the following parameters: kinematic viscosity of  $\text{H}_2\text{O}$  at 25  $^\circ\text{C}$ ,  $0.01 \text{ cm}^2 \text{ s}^{-1}$ ; solubility of  $\text{O}_2$  in air-saturated 1 M  $\text{HClO}_4$ , 0.24 mM; diffusion coefficient of  $\text{O}_2$ ,  $1.7 \times 10^{-5} \text{ cm}^2 \text{ s}^{-1}$ .<sup>22</sup> The solubility of dioxygen in 1 M  $\text{HClO}_4$  was calculated by using the Setschenow equation ( $\ln\{m_{\text{O}_2}^0/m_{\text{O}_2}\} = k_s \times m$ ) and the Pitzer equation<sup>25</sup> ( $k_s(\text{HClO}_4) = 2\lambda_{\text{O}_2,\text{H}^+} + 2\lambda_{\text{O}_2,\text{ClO}_4^-}$ ) where  $m$  is the molality ( $\text{mol kg}^{-1}$ ) of  $\text{HClO}_4$ ,  $m_{\text{O}_2}^0$  is the molality of  $\text{O}_2$  in pure water,<sup>26</sup>  $\lambda_{\text{O}_2,\text{H}^+} = 0.0353$ , and  $\lambda_{\text{O}_2,\text{ClO}_4^-} = -0.007$ .<sup>27</sup>

## Results and Discussion

**Redox Properties of Complexes 1a, 2, and 3a and Catalytic Reduction of  $\text{O}_2$ .** A detailed discussion is given for compounds **1a**, **2**, and **3a**, and this is followed by data on the other linked derivatives in the two series of biscobalt complexes.

The three series of cobalt complexes were applied to an edge-plane pyrolytic graphite (EPG) electrode by irreversible adsorption from a dilute chloroform solution. Cyclic voltammograms recorded at a graphite disk coated with complex **1a** are illustrated in Figure 1A. In the absence of dioxygen, the response of the modified graphite electrode is characterized by a redox process centered at  $E_{1/2} = 0.38$  V in 1 M  $\text{HClO}_4$  ( $E_{\text{pc}} = 0.36$  V,  $E_{\text{pa}} = 0.40$  V). When the solution is saturated with air, a larger cathodic peak is observed at almost the same potential of  $E_p = 0.40$  V. The reduction of  $\text{O}_2$  at an uncoated graphite electrode occurs at  $E_p = -0.34$  V which indicates that complex **1a** catalyzes the electroreduction of dioxygen when adsorbed on graphite.

A catalytic reduction wave of dioxygen is also observed at a rotating platinum ring–graphite disk electrode modified by adsorption of complex **1a** on the disk as illustrated in Figure 1B. This RRDE voltammogram was obtained by scanning the disk potential from 0.70 to 0.00 V vs SCE at a rotation speed of 100 rpm while holding the ring potential at 1.10 V so that any  $\text{H}_2\text{O}_2$  formed at the disk could be detected at the ring. Under these conditions, the anodic ring current results from the

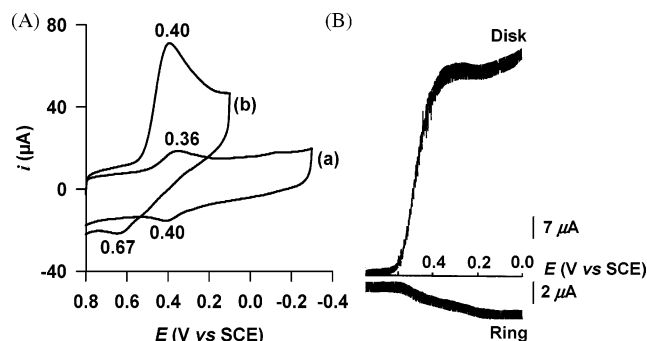


**Figure 1.** (A) Cyclic voltammograms of **1a** adsorbed on an EPG electrode. Supporting electrolyte: 1 M  $\text{HClO}_4$  (a) saturated with argon and (b) saturated with air. Scan rate:  $50 \text{ mV s}^{-1}$ . (B) Reduction of  $\text{O}_2$  at a rotating ring (Pt)–disk (EPG) electrode in air-saturated 1 M  $\text{HClO}_4$ . The potential of the ring electrode was maintained at 1.1 V. Rotation rate: 100 rpm. Scan rate:  $5 \text{ mV s}^{-1}$ .

**Table 1.** Electroreduction of Dioxygen by Adsorbed Dicobalt Porphyrin–Corroles and Biscorroles in Air-Saturated 1 M  $\text{HClO}_4$

compd		$E_p^a$	$E_{1/2}^b$	$n^c$
<b>1a</b>	$(\text{PCA})\text{Co}_2$	0.40	0.47	3.9
<b>1b</b>	$(\text{PCB})\text{Co}_2$	0.38	0.46	3.7
<b>1c</b>	$(\text{PCX})\text{Co}_2$	0.38	0.45	3.7
<b>1d</b>	$(\text{PCO})\text{Co}_2$	0.34	0.41	3.5
<b>2</b>	$(\text{Me}_4\text{Ph}_5\text{Cor})\text{Co}$	0.36	0.38	2.9
<b>3a</b>	$(\text{BCA})\text{Co}_2$	0.36	0.39	3.4
<b>3b</b>	$(\text{BCB})\text{Co}_2$	0.35	0.37	2.4
<b>3c</b>	$(\text{BCX})\text{Co}_2$	0.34	0.37	2.9
<b>3d</b>	$(\text{BCO})\text{Co}_2$	0.33	0.35	3.4
<b>3e</b>	$(\text{BCS})\text{Co}_2$	0.33	0.35	3.1

<sup>a</sup> Peak potential of the dioxygen reduction wave (V vs SCE). <sup>b</sup> Half-wave potential (V vs SCE) for dioxygen reduction at rotating disk electrode ( $\omega = 100 \text{ rpm}$ ). <sup>c</sup> The apparent number of electrons transferred per dioxygen molecule ( $n$ ) at  $E_{1/2}$  is calculated from  $n = 4I_D/(I_D + I_R/N)$  where  $I_D$  and  $I_R$  are disk and ring currents, respectively, and  $N$  ( $= 0.24$ ) is the collection efficiency of the ring–disk electrode.<sup>21</sup>

oxidation of  $\text{H}_2\text{O}_2$  to  $\text{O}_2$ . As seen in the figure, the disk current begins to increase at about 0.60 V, and the plateau is reached at 0.30 V. At about 0.26 V, the current begins to decrease slightly and then rises again as the potential is scanned to more negative values. A similar behavior was previously observed for  $(\text{FTF4})\text{Co}_2$ <sup>28,29</sup> (FTF4 = face-to-face porphyrin dimer with a linking group of 4 atoms) and biscobalt “Pacman” type bisporphyrins.<sup>10,30,31</sup> Only a relatively small amount of hydrogen peroxide is detected at the ring electrode in the vicinity of  $E_{1/2}$  when the reaction is carried out in air-saturated  $\text{HClO}_4$  (Table 1). The value of the disk current at  $E_{1/2}$  corresponds to an apparent number of electrons transferred of  $n = 3.9$ . From the data in the figure, we cannot say which of the two cobalt centers is reduced first in  $(\text{PCA})\text{Co}_2$  (that of the corrole or that of the porphyrin), but there is no doubt that the redox process at  $E_{1/2} = 0.38$  V in  $\text{HClO}_4$  under argon corresponds to the electroreduction of  $\text{O}_2$  to give  $\text{H}_2\text{O}$  at  $E_p = 0.40$  V under air.

The electrochemical and electrocatalytic properties of the monocorrole **2** in  $\text{HClO}_4$  differ from that of the dicobalt porphyrin–corrole **1a** under the same solution conditions. The

- (22) Shi, C.; Anson, F. C. *Inorg. Chem.* **1998**, *37*, 1037–1043.  
 (23) Conway, B. E.; Angerstein-Kozłowska, H.; Sharp, W. B. A.; Criddle, E. *Anal. Chem.* **1973**, *45*, 1331–1336.  
 (24) Hsueh, K.-L.; Gonzalez, E. R.; Srinivasan, S. *Electrochim. Acta* **1983**, *28*, 691–697.  
 (25) Millero, F. J.; Huang, F. J. *Chem. Eng. Data* **2003**, *48*, 1050–1054.  
 (26) Millero, F. J.; Huang, F.; Laferiere, A. L. *Geochim. Cosmochim. Acta* **2002**, *66*, 2349–2359.  
 (27) Clegg, S. L.; Brimblecombe, P. *Geochim. Cosmochim. Acta* **1990**, *54*, 3315–3328.

- (28) Collman, J. P.; Marrocco, M.; Denisevich, P.; Koval, C.; Anson, F. C. *J. Electroanal. Chem.* **1979**, *101*, 117–122.  
 (29) Collman, J. P.; Denisevich, P.; Konai, Y.; Marrocco, M.; Koval, C.; Anson, F. C. *J. Am. Chem. Soc.* **1980**, *102*, 6027–6036.  
 (30) Liu, H.-Y.; Abdalmuhdi, I.; Chang, C. K.; Anson, F. C. *J. Phys. Chem.* **1985**, *89*, 665–670.  
 (31) Chang, C. J.; Deng, Y.; Shi, C.; Chang, C. K.; Anson, F. C.; Nocera, D. G. *Chem. Commun.* **2000**, 1355–1356.



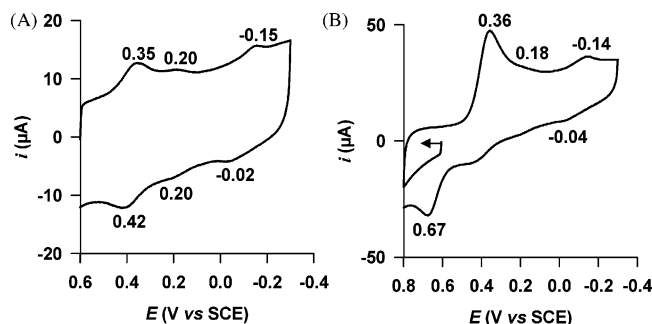


**Figure 2.** Cyclic voltammograms of **2** adsorbed on EPG electrode. Supporting electrolyte: 1 M HClO<sub>4</sub> saturated (A) with argon, (B) with air. Scan rate: 50 mV s<sup>-1</sup>.

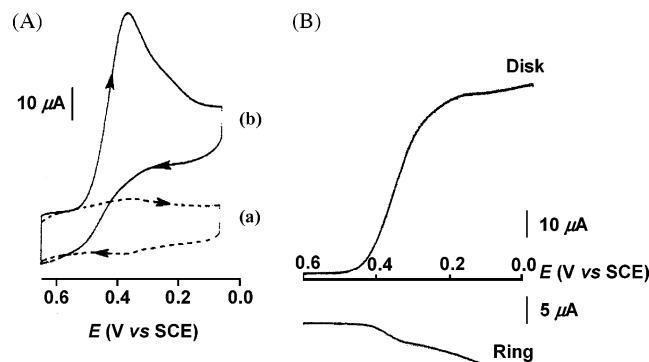


**Figure 3.** (A) Cyclic voltammograms of **3a** adsorbed on an EPG electrode. Supporting electrolyte: 1 M HClO<sub>4</sub> (a) saturated with argon and (b) saturated with air. Scan rate: 50 mV s<sup>-1</sup>. (B) Reduction of O<sub>2</sub> at a rotating ring (Pt)-disk (EPG) electrode in air-saturated 1 M HClO<sub>4</sub>. The potential of the ring electrode was maintained at 1.1 V. Rotation rate: 100 rpm. Scan rate: 5 mV s<sup>-1</sup>.

cyclic voltammogram of **2** adsorbed on a graphite disk in the absence of dioxygen shows three reversible processes located at  $E_{1/2} = 0.38, 0.20$ , and  $-0.08$  V (Figure 2A). The three reactions can be related to similar reactions for the same compound in CH<sub>2</sub>Cl<sub>2</sub> which occur at  $E_{1/2} = 0.62, 0.45$ , and  $-0.15$  V.<sup>14,17</sup> The electrochemical response at  $-0.15$  V was assigned to the Co(III)/Co(II) couple.<sup>17</sup> In comparison with the same process of a structurally related porphyrin, (OEP)Co<sup>32</sup> ( $E_{1/2} = 0.41$  V) where OEP = octaethylporphyrin, the smaller ring size of the macrocyclic cavity<sup>33</sup> of **2** shifts the formal potential of the Co(III)/Co(II) couple by 490 mV to lower values in accordance with the fact that a corrole macrocycle stabilizes the Co(III) oxidation state whereas porphyrins stabilize cobalt in a +2 oxidation state.<sup>1,33,34</sup> The two processes at  $E_{1/2} = 0.38$  and  $0.20$  V for complex **2** suggest reduction via a dimeric species as is also observed in a nonaqueous solvent such as CH<sub>2</sub>Cl<sub>2</sub>.<sup>14,17</sup> The first reduction peak at  $E_p = 0.35$  V in Figure 2A thus probably corresponds to formation of a monooxidized dimer, [(**2**)<sub>2</sub>]<sup>+</sup>, which is catalytically active toward the reduction of dioxygen as seen in Figure 2B by the substantially enhanced peak currents at  $E_p = 0.36$  V in the presence of O<sub>2</sub>.

Shown in Figure 3 are the cyclic voltammograms and rotating ring-disk electrode voltammograms responses obtained for (BCA)Co<sub>2</sub>, **3a**, adsorbed on an EPG electrode in 1 M HClO<sub>4</sub>. Results for the biscalcorole **3a** parallel what is observed for **1a**

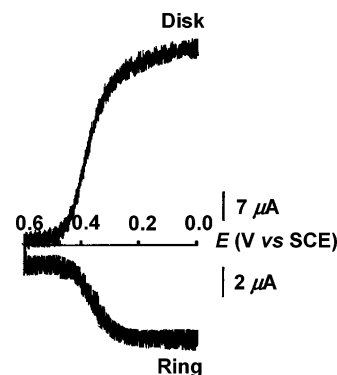


**Figure 4.** Reduction of O<sub>2</sub> at a rotating ring (Pt)-disk (EPG) electrode coated with **2** in air-saturated 1 M HClO<sub>4</sub>. Collection efficiency  $N = 0.24$ . The potential of the ring electrode was maintained at 1.1 V. Rotation rate: 100 rpm. Scan rate: 5 mV s<sup>-1</sup>.

except that more H<sub>2</sub>O<sub>2</sub> is produced at the  $E_{1/2}$  of 0.39 V (30%) than in the case of the porphyrin-corrrole mixed oxidation state derivative where only 5% of H<sub>2</sub>O<sub>2</sub> was observed. The biscalcorole **3a** is thus less selective than the porphyrin-corrrole dyad **1a** but more selective than the monocorrrole **2** (55% H<sub>2</sub>O<sub>2</sub>). In comparison with the dicobalt porphyrin-corrrole **1a** and biscalcorole **3a**, the half-wave potential  $E_{1/2}$  of the dioxygen reduction wave is less positive for the monomeric cobalt complex **2** (Table 1). Also, in the case of **2**, H<sub>2</sub>O<sub>2</sub> is detected at the ring electrode as soon as dioxygen reduction occurs (Figure 4). Under these conditions, the value of  $n$  calculated from the disk and the ring currents is 2.9 at 0.38 V (Table 1). As complex **2** is not catalytically active toward the reduction of H<sub>2</sub>O<sub>2</sub> (vide infra), this value of  $n$  requires that a portion of the dioxygen that reaches the electrode surface be reduced by four electrons to H<sub>2</sub>O. The catalytic behavior of **2** is thus similar to what has been reported for cobalt porphyrins with unsubstituted meso positions such as (OEP)Co<sup>32</sup> or Co(II) porphine.<sup>35</sup> In both cases, a formation of dimers on the surface of the graphite electrode was proposed to explain the catalytic electroreduction of O<sub>2</sub> to H<sub>2</sub>O.

**Kinetics of O<sub>2</sub> Reduction Catalyzed by (Me<sub>4</sub>Ph<sub>5</sub>Cor)Co, **2**, and (PCA)Co<sub>2</sub>, **1a**.** Figure 5A shows a set of current-potential curves for the reduction of dioxygen at a rotating disk electrode coated with the cobalt monocorrrole **2** and porphyrin-corrrole **1a** in 1 M HClO<sub>4</sub>. The corresponding Levich plot of limiting current vs the square root of the rotation rate ( $\omega$ )<sup>1/2</sup> and the lines calculated from the Levich equation for the diffusion-convection-limited two- and four-electron reduction of dioxygen are shown in Figure 5B. The Levich plot for monocorrrole **2** shows that the steady-state limiting currents exceed the calculated values corresponding to the two-electron reduction of O<sub>2</sub>. The nonlinearity of the Levich plot in Figure 5B suggests that the catalytic reaction is limited by a rate-determining step that precedes the electronic transfer (CE mechanism). This nonlinearity was previously observed for several cobalt(II) porphyrin complexes,<sup>22,32,36-41</sup> and the

(32) Song, E.; Shi, C.; Anson, F. C. *Langmuir* **1998**, *14*, 4315-4321.

(33) Erben, C.; Will, S.; Kadish, K. M. In *The Porphyrin Handbook*; Kadish, K. M., Smith, J. R. L., Guillard, R., Eds.; Academic Press: Boston, 2000; Vol. 2, pp 233-300.

(34) Licocchia, S.; Paolesse, R. *Struct. Bonding* **1995**, *84*, 71-133.

(35) Shi, C.; Steiger, B.; Yuasa, M.; Anson, F. C. *Inorg. Chem.* **1997**, *36*, 4294-4295.

(36) Durand, R. R., Jr.; Anson, F. C. *J. Electroanal. Chem.* **1982**, *134*, 273-289.

(37) Anson, F. C.; Ni, C.-L.; Saveant, J.-M. *J. Am. Chem. Soc.* **1985**, *107*, 3442-3450.

(38) Yuasa, M.; Steiger, B.; Anson, F. C. *J. Porphyrins Phthalocyanines* **1997**, *1*, 181-188.

(39) D'Souza, F.; Hsieh, Y.-Y.; Deviprasad, G. R. *Chem. Commun.* **1998**, 1027-1028.

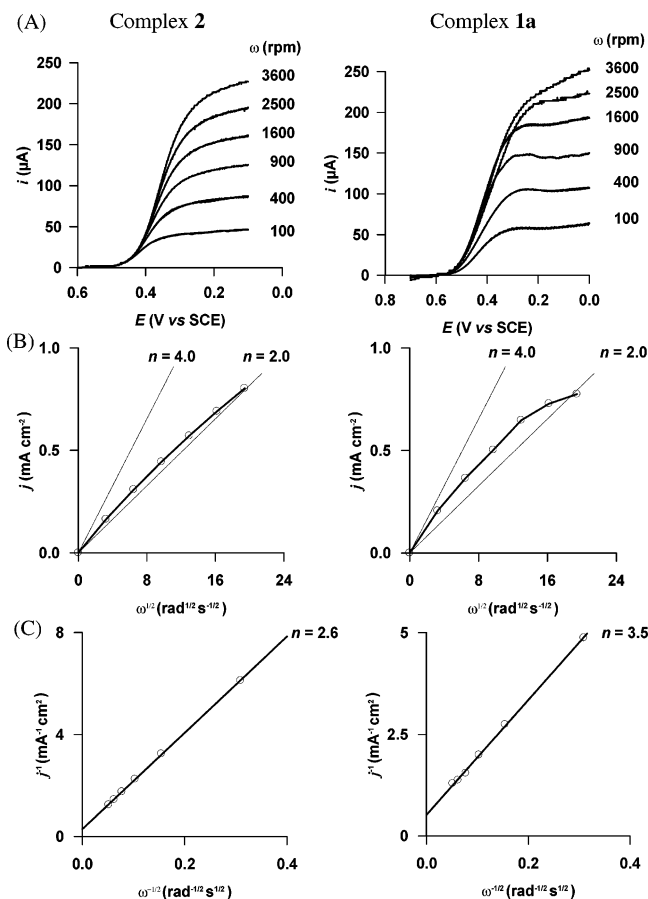


**Figure 5.** (A) Current–potential curves for the reduction of O<sub>2</sub> in 1 M HClO<sub>4</sub> at a rotating graphite disk electrode coated with 2.0 × 10<sup>-10</sup> mol cm<sup>-2</sup> of **2** (left) and 11.0 × 10<sup>-10</sup> mol cm<sup>-2</sup> of **1a** (right). Values of the rotational velocity (*ω*) of the electrode in rpm are indicated on each curve. The disk potential was scanned at 5 mV s<sup>-1</sup>. (B) Levich plots of the rotating limiting currents (*j*) of (A) (O) vs square root of rotational velocity (*ω*)<sup>1/2</sup>. The lines refer to the theoretical curves for the 2e<sup>-</sup> and 4e<sup>-</sup> processes, as indicated in the figures. (C) Koutecký–Levich plots corresponding to B.

chemical step was assigned to the formation of a dioxigen adduct<sup>42</sup> which is a reducible species. Kinetic analysis of such systems is facilitated by means of Koutecký–Levich plots<sup>43</sup> of reciprocal current density (*j*<sub>lim</sub>)<sup>-1</sup> vs reciprocal square root of rotational velocity (*ω*)<sup>-1/2</sup>. Typical plots are shown in Figure 5C. These plots are interpreted on the basis of eq 1:

$$\frac{1}{j_{\text{lim}}} = \frac{1}{j_{\text{lev}}} + \frac{1}{j_k} \quad (1)$$

where *j*<sub>lim</sub> is the measured limiting current density (mA cm<sup>-2</sup>). The Levich current, *j*<sub>lev</sub>, and the kinetic current, *j*<sub>k</sub>, that measure the rate of the current-limiting chemical reaction, are defined by eqs 2 and 3, respectively.

$$j_{\text{lev}} = 0.62nFD^{2/3}v^{-1/6}C^*\omega^{1/2} \quad (2)$$

where *n* is the number of electrons transferred in the overall electrode reaction, *F* the Faraday constant (96485 C mol<sup>-1</sup>), *D* and *C*<sup>\*</sup> are the diffusion coefficient (cm<sup>2</sup> s<sup>-1</sup>) and bulk

**Table 2.** Rate Constants (*k*) for the Electroreduction of O<sub>2</sub> by Adsorbed Catalysts in Air-Saturated Aqueous Acidic Solution (pH = 0)

catalyst	10 <sup>-5</sup> <i>k</i> , M <sup>-1</sup> s <sup>-1</sup>	ref <sup>a</sup>
(PCA)Co <sub>2</sub> ( <b>1a</b> )	0.2	T.W.
(Me <sub>4</sub> Ph <sub>5</sub> Cor)Co ( <b>2</b> )	5.7	T.W.
(FTF4)Co <sub>2</sub>	3.0	42
(diethylesterMe <sub>2</sub> Et <sub>2</sub> P)Co	1.4	42
(DPA)Co <sub>2</sub>	0.2	30

<sup>a</sup> T.W. = This work.

concentration of dioxigen (mol dm<sup>-3</sup>), respectively, *v* is the kinematic viscosity of water (cm<sup>2</sup> s<sup>-1</sup>), and *ω* is the angular rotation speed (rad s<sup>-1</sup>) of the electrode.

$$j_k = 10^3 n F k \Gamma C^* \quad (3)$$

where *k* (M<sup>-1</sup> s<sup>-1</sup>) is the second-order rate constant governing the current-limiting reaction between the reduced catalyst and O<sub>2</sub>, and *Γ* (mol cm<sup>-2</sup>) is the surface concentration of catalyst on the electrode that participates in catalyzing the reaction. The quantity of (Me<sub>4</sub>Ph<sub>5</sub>Cor)Co present on the electrode (*Γ* = 2.0 × 10<sup>-10</sup> mol cm<sup>-2</sup>) was obtained by measuring the area under the cyclic voltammogram recorded in dioxigen-free 1 M HClO<sub>4</sub>. The value of *n* determined from the slope of the Koutecký–Levich plot (Figure 5C) shows that a portion of dioxigen is reduced to water. This is in agreement with the value of *n* = 2.9 determined from the ring–disk experiment at a rotation speed of 100 rpm (Table 1). The value of the O<sub>2</sub> reduction rate constant *k*, evaluated at pH = 0, from the intercept of the Koutecký–Levich plot, is higher than previously reported rate constants governing the kinetics of the coordination of dioxigen to adsorbed cobalt(II) porphyrin complexes (Table 2).<sup>42</sup>

The rotating disk procedure described above for measuring the rate constant governing the catalytic reaction of **2** with O<sub>2</sub> was also applied to the dicobalt porphyrin–corrole **1a**. An EPG disk was modified with (PCA)Co<sub>2</sub> using a dip-coating procedure (vide supra). The surface coverage of the disk was calculated from integration of the voltammetric peak recorded in a deoxygenated acidic solution (Figure 1A) and was found to be 11.0 × 10<sup>-10</sup> mol cm<sup>-2</sup> of geometric electrode area. The recorded hydrodynamic voltammograms in the presence of dioxigen are shown in Figure 5A. The Levich plot in Figure 5B is nonlinear, as expected for a reduction in which a current-limiting chemical step precedes the electron transfer. The reciprocal slope of the corresponding Koutecký–Levich plot (Figure 5C) corresponds to an apparent *n* value of 3.5 which suggests that O<sub>2</sub> is reduced to a mixture of H<sub>2</sub>O and H<sub>2</sub>O<sub>2</sub>. This is also consistent with the magnitudes of the anodic ring currents at potentials on the plateau of the disk current–potential curve in Figure 1B. The rate constant, *k*, for the catalytic reduction of O<sub>2</sub> by (PCA)Co<sub>2</sub> was evaluated from the intercept of the Koutecký–Levich plot (Figure 5C) and found to be 0.2 × 10<sup>5</sup> M<sup>-1</sup> s<sup>-1</sup> (Table 2). This value is lower than that obtained for the monocobalt porphyrin (diethylesterMe<sub>2</sub>Et<sub>2</sub>P)Co (*k* = 1.4 × 10<sup>5</sup> M<sup>-1</sup> s<sup>-1</sup>)<sup>42</sup> and its related dimer (FTF4)Co<sub>2</sub> (*k* = 3.0 × 10<sup>5</sup> M<sup>-1</sup> s<sup>-1</sup>),<sup>42</sup> but it is identical to that reported previously for the electrocatalytic reduction of O<sub>2</sub> in 1 M CF<sub>3</sub>CO<sub>2</sub>H by a (DPA)-Co<sub>2</sub>-coated graphite electrode where DPA = anthracenyl-bridged diporphyrin (*k* = 0.2 × 10<sup>5</sup> M<sup>-1</sup> s<sup>-1</sup>).<sup>30</sup>

**Thin-Layer Voltammetry.** Further insight into the catalyzed reduction of dioxigen by **2** was obtained by dissolving the

(40) Steiger, B.; Anson, F. C. *Inorg. Chem.* **2000**, *39*, 4579–4585.

(41) Shi, C.; Anson, F. C. *Inorg. Chem.* **2001**, *40*, 5829–5833.

(42) Durand, R. R., Jr.; Bencosme, C. S.; Collman, J. P.; Anson, F. C. *J. Am. Chem. Soc.* **1983**, *105*, 2710–2718.

(43) Treimer, S.; Tang, A.; Johnson, D. C. *Electroanalysis* **2002**, *14*, 165–171.

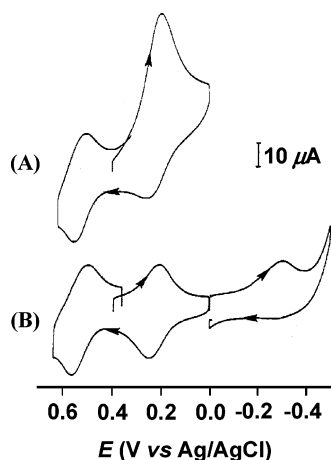


**Figure 6.** Cyclic voltammograms of **2** (0.6 mM) dissolved in a thin layer of acidified PhCN placed on an EPG electrode that was immersed in 1 M HClO<sub>4</sub>. (A) In the presence of O<sub>2</sub> and (B) after the aqueous phase (and the equilibrated thin layer of PhCN) was saturated with argon. Scan rate: 50 mV s<sup>-1</sup>.

catalyst in a thin layer of benzonitrile next to the electrode instead of adsorbing it directly on the electrode surface. Shown in Figure 6 are cyclic voltammograms obtained with an EPG electrode on which was placed a 30 μm layer of benzonitrile containing (Me<sub>4</sub>Ph<sub>5</sub>Cor)Co. The electrode was immersed in an aqueous solution of 1 M HClO<sub>4</sub>. The large cathodic peak current at  $E_p = 0.20$  V vs Ag/AgCl (Figure 6A) arises from the reduction of O<sub>2</sub> catalyzed by **2**. The rise in the catalytic current occurs at the same potential where, in the absence of O<sub>2</sub>, [(Me<sub>4</sub>Ph<sub>5</sub>Cor)Co<sup>IV</sup>]<sup>+</sup> is reduced to [(Me<sub>4</sub>Ph<sub>5</sub>Cor)Co<sup>III</sup>]<sup>0</sup> in 1 M HClO<sub>4</sub> (Figure 6B). This implicates the cobalt(III) corrole as the catalytically active species. The reversible process observed at more cathodic potentials ( $E_p = -0.30$  V vs Ag/AgCl) corresponds to the Co(III)/Co(II) redox couple.

**Catalytic Activity of Cobalt Corrole Derivatives toward H<sub>2</sub>O<sub>2</sub> at pH = 0.** As shown by the rotating disk electrode voltammograms of (Me<sub>4</sub>Ph<sub>5</sub>Cor)Co (Figure 5A), the reduction of O<sub>2</sub> proceeds in a single step, and H<sub>2</sub>O<sub>2</sub> is the major product of the reduction at the plateau. In contrast, the larger disk current with (PCA)Co<sub>2</sub> (Figure 5A) shows that a portion of the O<sub>2</sub> is reduced to H<sub>2</sub>O instead of H<sub>2</sub>O<sub>2</sub>. However, the catalyst may produce H<sub>2</sub>O<sub>2</sub> as an intermediate species in the catalytic process. To test this possibility, the solution used to record the cyclic voltammogram in the presence of dioxygen (Figure 1) was made 0.5 mM in H<sub>2</sub>O<sub>2</sub> and deoxygenated with argon for 20 min. The cyclic voltammogram recorded with a (PCA)Co<sub>2</sub>-coated electrode in the presence of hydrogen peroxide is shown in Figure 7A. A catalytic oxidation peak of H<sub>2</sub>O<sub>2</sub> to O<sub>2</sub> was observed at 0.65 V, whereas the reduction of the dioxygen formed at the electrode occurred at 0.42 V. No peak corresponding to the reduction of H<sub>2</sub>O<sub>2</sub> to H<sub>2</sub>O was detected between 0.80 and 0.00 V. The same electrochemical behavior was observed for (Me<sub>4</sub>Ph<sub>5</sub>Cor)Co (Figure 7B) except that the magnitude of the oxidation peak current at 0.70 V was relatively higher than that of (PCA)Co<sub>2</sub>. For a more quantitative assessment of the catalytic properties of complexes **1a** and **2** toward H<sub>2</sub>O<sub>2</sub>, current–potential curves were recorded at a rotating disk electrode in 1 M HClO<sub>4</sub> saturated with argon (Figure 8). Both adsorbed complexes catalyze the electrooxidation of H<sub>2</sub>O<sub>2</sub> at  $E_{1/2} = 0.61$  and 0.65 V, respectively. The decline in the limiting currents observed for **1a** and **2** at potentials higher than 0.80 V

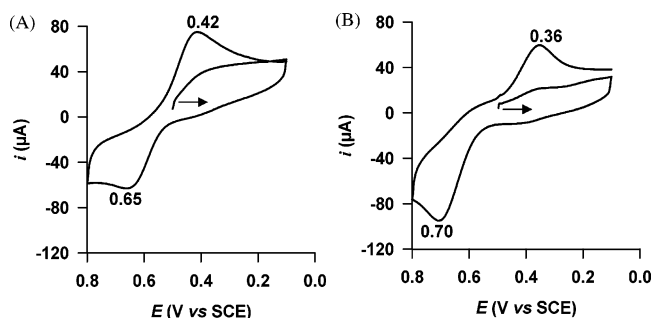


**Figure 7.** Cyclic voltammograms of **1a** (A) and **2** (B) adsorbed on EPG electrode. Supporting electrolyte: 1 M HClO<sub>4</sub> saturated with argon. [H<sub>2</sub>O<sub>2</sub>] = 0.5 mM. Scan rate: 50 mV s<sup>-1</sup>.

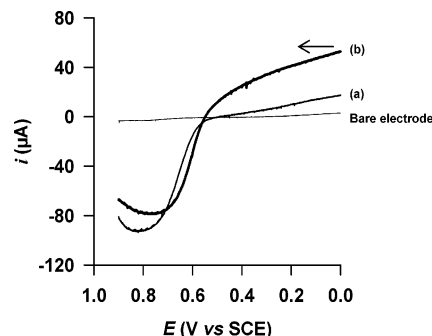


**Figure 8.** Rotating disk voltammograms of **2** (curve a) and **1a** (curve b) adsorbed on EPG electrode. Supporting electrolyte: 1 M HClO<sub>4</sub> saturated with argon. [H<sub>2</sub>O<sub>2</sub>] = 0.5 mM. Rotation rate: 100 rpm. Scan rate: 5 mV s<sup>-1</sup>.

corresponds to a gradual loss of catalytic activity due to a possible degradation at the EPG surface. The curves for reduction of H<sub>2</sub>O<sub>2</sub> examined at the (Me<sub>4</sub>Ph<sub>5</sub>Cor)Co-coated electrode reveal that cobalt(III) monocorrole **2** reduces H<sub>2</sub>O<sub>2</sub> at a much lower rate than it catalyzes its oxidation. The RDE voltammogram recorded in a deoxygenated solution containing 0.5 mM H<sub>2</sub>O<sub>2</sub> (curve a, Figure 8) shows a slow rise of the disk current from ca. 0.60 to 0.00 V. An analogous RDE experiment with a (PCA)Co<sub>2</sub>-coated graphite disk (curve b, Figure 8) shows a relatively similar behavior of the dicobalt porphyrin–corrole dyad toward the catalytic reduction of H<sub>2</sub>O<sub>2</sub>. However, the magnitude of the cathodic currents recorded between 0.60 and 0.00 V are higher than that observed for the monocobalt corrole (Me<sub>4</sub>Ph<sub>5</sub>Cor)Co (curve a, Figure 8). As expected, no oxidations or reductions of H<sub>2</sub>O<sub>2</sub> were observed at the bare electrode, and this is also illustrated in Figure 8.

Collman et al. observed that a graphite electrode coated with (FTF4)Co<sub>2</sub> also catalyzes the two-electron reduction of H<sub>2</sub>O<sub>2</sub> to H<sub>2</sub>O in acidic media.<sup>44</sup> The catalytic reduction of H<sub>2</sub>O<sub>2</sub> by (FTF4)Co<sub>2</sub> was characterized by rotating disk electrode voltammograms similar to those recorded for complex **1a** (Figure 8). A similar catalytic activity toward H<sub>2</sub>O<sub>2</sub> was reported by Anson, Chang, and co-workers for a dicobalt cofacial diporphyrin, (DPA)Co<sub>2</sub>, that is structurally similar to complex **1a**.<sup>30</sup> The lack of significant catalytic activity of (DPA)Co<sub>2</sub> toward the disproportionation of H<sub>2</sub>O<sub>2</sub> was also demonstrated. Both Collman and Anson have stated that the rate of the electrocatalytic reduction of H<sub>2</sub>O<sub>2</sub> by (FTF4)Co<sub>2</sub> and (DPA)Co<sub>2</sub> is very slow compared to the rate of O<sub>2</sub> reduction.<sup>30,44</sup> From

(44) Collman, J. P.; Hendricks, N. H.; Leidner, C. R.; Ngameni, E.; L'Her, M. *Inorg. Chem.* **1988**, 27, 387–393.

the results shown in Figure 8 it is clear that this is also true for (PCA)Co<sub>2</sub>.

**Effect of Different Spacers on O<sub>2</sub> Catalysis.** The dioxygen reduction catalytic properties of dicobalt porphyrin–corrole and biscalloles complexes bridged by biphenylene, 9,9-dimethylxanthene, dibenzofuran, and dibenzothiophene were compared to those of (PCA)Co<sub>2</sub> and (BCA)Co<sub>2</sub> (Chart 1). The electrochemical data are compiled in Table 1. The structural details on complexes with spacers of the type used in this study were reported previously.<sup>18,45–47</sup> The rigidity of the anthracene and biphenylene bridges in complexes **1a**, **1b**, **3a**, and **3b** minimize ring lateral slippage while maintaining a face-to-face arrangement of both macrocycles.<sup>8</sup> Biphenylene provides a tighter binding cavity than anthracene due to the fewer number of atoms separating the macrocyclic units. However, both single rigid linkers afford a small flexibility along the longitudinal axis of the ligands that allow the molecular clefts to structurally accommodate reaction intermediates during multielectron catalysis (“Pac-Man” effect<sup>8,48</sup>), resulting in an efficient catalytic reduction of O<sub>2</sub>. The porphyrin–corrole dyads bridged by 9,9-dimethylxanthene (**1c**) and dibenzofuran (**1d**) also catalyze efficiently the direct four-electron reduction of O<sub>2</sub> to H<sub>2</sub>O (Table 1) despite the structural difference between the two ligands. The xanthene bridge contains the same number of atoms as anthracene, whereas the five-membered ether ring in dibenzofuran increases the size of the binding pocket. The presence of an sp<sup>3</sup> oxygen in the latter bridge allows the molecular system to open and close its binding pocket by a longitudinal distance of over 4 Å in the presence of exogenous ligands as reported by Nocera et al.<sup>48</sup> This longitudinal flexibility is also observed in the case of complex **1d** since the PCO system displays four-electron reactivity toward dioxygen (Table 1).

Coatings of cobalt(III) biscalloles catalyze O<sub>2</sub> reduction at more negative potentials than do the (PCY)Co<sub>2</sub> systems (Table

1). The  $E_{1/2}$  values of **3a–3c** are close to that observed for (Me<sub>4</sub>Ph<sub>5</sub>Cor)Co ( $E_{1/2}$  = 0.38 V), whereas complexes **3d** and **3e** reduce O<sub>2</sub> at more slightly negative potentials ( $E_{1/2}$  = 0.35 V). Rotating ring–disk measurements show that the reduction of O<sub>2</sub> by (BCY)Co<sub>2</sub> complexes produces a more significant amount of H<sub>2</sub>O<sub>2</sub> than that by porphyrin–corrole derivatives. In comparison with (PCY)Co<sub>2</sub> systems, the decrease of catalytic selectivity toward four-electron reduction of O<sub>2</sub> to H<sub>2</sub>O in 1 M HClO<sub>4</sub> observed with (BCY)Co<sub>2</sub>-coated electrodes suggests that the partially reduced dioxygen species is less stabilized. This decrease of selectivity for the direct reduction of O<sub>2</sub> to H<sub>2</sub>O may be also explained by the difference of electronic properties between the electron-poor aryl-substituted corrole and the electron-rich alkyl-substituted porphyrin subunits. In comparison with **1**, the presence of a second cobalt(III) corrole unit in **3** may reduce the basicity of the oxygen adduct which strongly disfavors the four-electron pathway.<sup>7</sup>

## Conclusions

In summary, we have shown that cobalt corroles can be used as effective catalysts in the reduction of O<sub>2</sub>. The onset of dioxygen reduction occurs between 0.33 and 0.40 V for the 10 investigated catalysts when measured by cyclic voltammetry in 1 M HClO<sub>4</sub>. However, the H<sub>2</sub>O/H<sub>2</sub>O<sub>2</sub> product ratios of the reduction differ in each case, with the most effective catalyst being the mixed oxidation state derivative **1a–1d** which leads almost exclusively to a four-electron reduction of O<sub>2</sub> at  $E_{1/2}$  = 0.41–0.47 V vs SCE. A four-electron reduction also occurs to some extent in the absence of a porphyrin macrocycle; under these conditions O<sub>2</sub> reduction occurs at an  $E_{1/2}$  of 0.35–0.39 V as seen in Table 1. Finally, reduction of hydrogen peroxide in 1 M HClO<sub>4</sub> by the dicobalt porphyrin–corrole **1a** is too slow to account for participation of free H<sub>2</sub>O<sub>2</sub> as an intermediate in the four-electron reduction of O<sub>2</sub>.

**Acknowledgment.** K.M.K. is grateful to the Robert A. Welch Foundation (Grant E-680) for support of this research as is L.K. for a predoctoral fellowship. The Région Bourgogne and CNRS are also acknowledged for financial support and for a BDI fellowship (F.B.).

JA0501060

- (45) Kadish, K. M.; Burdet, F.; Jerome, F.; Barbe, J.-M.; Ou, Z.; Shao, J.; Guillard, R. *J. Organomet. Chem.* **2002**, 652, 69.
- (46) Barbe, J.-M.; Stern, C.; Pacholska, E.; Espinosa, E.; Guillard, R. *J. Porphyrins Phthalocyanines* **2004**, 8, 301–312.
- (47) Guillard, R.; Gros, C. P.; Barbe, J.-M.; Espinosa, E.; Jerome, F.; Tabard, A.; Latour, J.-M.; Shao, J.; Ou, Z.; Kadish, K. M. *Inorg. Chem.* **2004**, 43, 7441–7455.
- (48) Deng, Y.; Chang, C. J.; Nocera, D. G. *J. Am. Chem. Soc.* **2000**, 122, 410–411.